we can rewrite (A4)

$$\frac{\partial F_r}{\partial x}+\frac{\partial F_i}{\partial y}=\left(\frac{\partial F_r}{\partial z}+\frac{\partial F_r}{\partial z^*}\right)+j\left(\frac{\partial F_i}{\partial z}-\frac{\partial F_i}{\partial z^*}\right)$$
$$=\frac{\partial F}{\partial z}+\frac{\partial F^*}{\partial z^*}=2\,\mathrm{Re}\,\frac{\partial F}{\partial z} \qquad \text{(A8)}$$

and (A5)

$$\begin{vmatrix}\partial F_r/\partial x & \partial F_r/\partial y\\ \partial F_i/\partial x & \partial F_i/\partial y\end{vmatrix}=\begin{vmatrix}\partial F_r/\partial z+\partial F_r/\partial z^* & j\frac{\partial F_r}{\partial z}-j\frac{\partial F_r}{\partial z^*}\\ \partial F_i/\partial z+\partial F_i/\partial z^* & j\frac{\partial F_i}{\partial z}-j\frac{\partial F_i}{\partial z^*}\end{vmatrix}$$
$$=2j\begin{vmatrix}\partial F_r/\partial z & \partial F_r/\partial z-\partial F_r/\partial z^*\\ \partial F_i/\partial z & \partial F_i/\partial z-\partial F_i/\partial z^*\end{vmatrix}$$
$$=-2\begin{vmatrix}\partial F/\partial z & \partial F/\partial z^*\\ \partial F_i/\partial z & \partial F_i/\partial z^*\end{vmatrix}$$
$$=\begin{vmatrix}\partial F/\partial z & \partial F/\partial z^*\\ \partial F^*/\partial z & \partial F^*/\partial z^*\end{vmatrix}. \qquad \text{(A9)}$$

From the above results, the concise expression for stability criterion (10) is deduced.

B. The Relation between the Coefficient B_v and the Locked Phase Difference θ

Let the oscillator admittance be given by

$$Y(j\omega,|V|^2)=Y_n+jB_\omega\,\Delta\omega+Y_v|V|^2 \qquad \text{(A10)}$$

and let us derive the microwave injection-locking equation.

In the case of a small signal $|b|$, we obtain from (3)–(5) and (8) [3]

$$\left[\frac{Y_{|V_0|}}{\sqrt{Y_0}}\{\Delta|a|+|b|\cos(\beta-\alpha)\}+Y_{j\omega}\cdot(j\Delta\omega+d/dt)\right]a=2Y_0\cdot b. \qquad \text{(A11)}$$

If the oscillator is adjusted to produce the maximum output power at the free-running state ($\hat{G}_0=2$), the real part of (A11) becomes zero [3]. Noting that $a^{-1}\,da/dt=|a|^{-1}d|a|/dt+j\,d\alpha/dt$, the imaginary part gives

$$\frac{d\alpha}{dt}=\frac{2Y_0}{B_\omega}\sqrt{1+(B_v/G_v)^2}\left|\frac{b}{a}\right|\sin(\beta-\alpha-\theta)-\Delta\omega \qquad \text{(A12)}$$

where

$$\theta=\arctan(B_v/G_v)$$

C. Geometrical Meaning of the Locking Phase Difference

$$\theta=\arctan(B_v/G_v)$$

We assume that the oscillator admittance is given by (A10) and that the oscillator is adjusted to generate the maximum output power in the free-running state ($G_0=2Y_0$). When a load $Y_L=G_L+jB_L$ is connected to the oscillator, we have

$$Y(j\omega,|V|^2)+Y_L=0. \qquad \text{(A13)}$$

If the load is matched to the transmission line ($Y_L=Y_0$), the above equation becomes identical to (4).

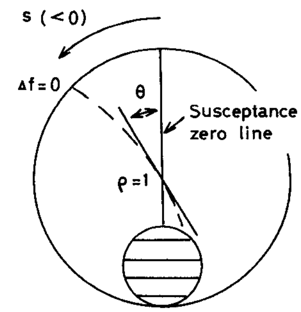

Fig. 8. Geometrical meaning of the injection-locking phase-difference θ on the Rieke diagram.
($\tan\theta=B_v/G_v=-S$, when $G_0=2Y_0$.)

We denote the normalized susceptance by S, on which the locus $\Delta\omega=0$ crosses the zero conductance locus (peripheral circle). Noting that $Y_L=jSY_0$, (A13) becomes

$$Y(j\omega_0,|V_1|^2)+jSY_0=0. \qquad \text{(A14)}$$

Eliminating B_0, $|V_0|^2$, and $|V_1|^2$ from (4) and (A14), we obtain

$$\tan\theta=B_v/G_v=-S.$$

By the principle of conformal mapping, θ is equal to the angle between the locus of $\Delta\omega=0$ and the zero-susceptance line at the point of the matched load ($Y_L=Y_0$), as is shown in Fig. 8.

Acknowledgment

The authors would like to thank H. Mizuno of Nippon Denso Co. Ltd. for his aid in the experiments.

References

[1] R. Adler, "A study of locking phenomena in oscillators," *Proc. IRE*, vol. 34, pp. 351–357, 1946.
[2] K. Kurokawa, *An Introduction to the Theory of Microwave Circuits*. New York: Academic Press, 1969.
[3] M. Nakajima and J. Ikenoue, "Locking phenomena in microwave oscillator circuits," *Int. J Electron*, vol. 44, pp. 465–472, 1978.
[4] K. Fukumoto, M. Nakajima, and J. Ikenoue, "Mathematical representation of microwave oscillator characteristics by use of the Rieke diagram," *IEEE Trans. Microwave Theory Tech.*, vol. MTT-31, pp. 954–959, 1983.

A New Cylindrical Electron Gun for Low-Power Tunable Gyrotrons with High Magnetic Compression Ratios

J. Y. L. MA

Abstract—**Because of the high magnetic compression ratio required, electrons in the Sydney University tunable gyrotron undergo multiple reflections before entering the resonant cavity. This results in unstable and**

Manuscript received April 3, 1984; revised November 19, 1984. This work was supported in part by the Australian Research Grants Scheme, the Australian Institute of Nuclear Science and Engineering, the Radio Research Board, the University of Sydney, and the Science Foundation for Physics.
The author is with the Wills Plasma Physics Department, School of Physics, University of Sydney, N.S.W. 2006, Australia.

0018-9480/85/0400-0323$01.00 ©1985 IEEE

unpredictable operation. A new cylindrical gun has been designed and fabricated. Computer simulations have predicted favorable broad-band behavior, and this has been confirmed by testing in the tunable gyrotron.

I. Introduction

The gyrotron has emerged as an important source of millimeter and submillimeter waves in recent years [1]–[3]. Its potential as a powerful and efficient source for electron cyclotron heating of thermonuclear fusion plasmas has attracted intensive research worldwide. The tunability aspect has offered the gyrotron as a powerful source for spectroscopy in the millimeter and far infrared regions.

The gyrotron consists of an electrooptical system which produces a hollow beam of electrons in helical motion, and a resonant cavity in which the electron beam interacts with and sustains a high-frequency microwave field. For efficient interaction, the electron beam radius R_0 has to match the location of the maximum electric field of the particular oscillating mode, and a large fraction of the electron energy should be in the transverse direction.

In the mainstream of high-power gyrotron research, the magnetron injection gun (MIG) has been used almost exclusively. Extensive computer codes have been developed to stimulate the MIG [4], [5]; however, the adiabatic theory of Gol'denberg *et al.* [6] serves to provide a convenient order of magnitude estimation. By the law of adiabatic invariance [7], we have

$$V_p^2/B = \text{const} \tag{1}$$

where V_p is the transverse velocity and B is the local magnetic field. The initial transverse velocity of the electron in a MIG-type gun is

$$V_{cp} = E_{cp}/B_c \tag{2}$$

where E_{cp} is the electric-field component at the cathode perpendicular to the magnetic field, and B_c is the magnetic field at the cathode. By applying (1) and using the initial transverse velocity of the electron as given in (2), the transverse velocity of the electron at the cavity is given by

$$V_{0p} = \sqrt{\alpha}\,(E_{cp}/B_c) \tag{3}$$

where $\alpha = B_0/B_c$ is the magnetic compression ratio, and B_0 is the magnetic field at the cavity.

The guiding center of the electron is always on the surface of the same axisymmetric force tube of the magnetic field. A precise calculation by Gol'denberg and Pankratova [8] yields the following results with an accuracy of up to terms of order $(r_1/R_0)^2$:

$$R_0 = R/\sqrt{\alpha} \tag{4}$$

where r_1 is the electron larmor radius, R_0 is the radial coordinate of the electron guiding center, and R is that of the electron emission point.

For a fixed-frequency gyrotron, once the frequency and operating mode have been decided, R_0 can be determined from the field pattern of the mode. The cathode radius and the magnetic compression ratio α can be determined by using (4).

For a tunable gyrotron [9], the matter is more complicated, because as the magnetic field is varied, the operating mode changes and the electron dynamics (3) are also effected. However, the effect on the perpendicular velocity of the electrons can be compensated for by adjusting E_{cp}, which is controlled by the anode voltage. To facilitate tunability and to keep the device simple to operate, the following design philosophy was adopted. A large cavity is employed so that the mode density is high [9].

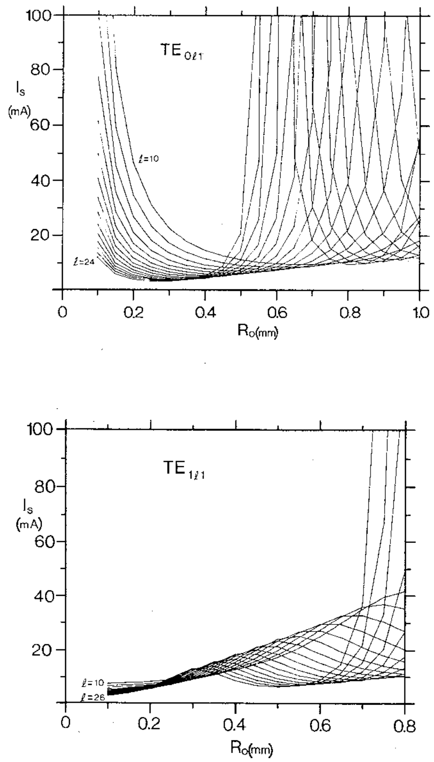

Fig. 1. Minimum starting current as a function of electron-beam radius R_0. The cavity has a radius of 11.69 mm and a length of 9.6 mm. The electron beam voltage is 20 kV and the electron velocity ratio is 1.5. (a) TE_{01} modes. (b) TE_{11} modes.

The modes are of high radial number, and the electric field has its greatest maximum at or near the axis of the cavity. Thus, it is possible to use an electron beam of small fixed radius such that most modes can be excited easily. Fig. 1 shows the minimum starting current versus electron beam radius R_0 as calculated from a linear theory [10]. It is seen that as long as R_0 is between 0.3 and 0.5 mm, all the TE_{01} and TE_{11} modes (for $l = 10$ to 24) can be excited with a starting current of no more than 30 mA.

II. Operation of the Tunable Gyrotron with a Conventional MIG

Gyrotron II, built at the University of Sydney, has generated frequencies in the range between 125 and 260 GHz in the modes from TE_{1101} to TE_{0201} [11]. The cavity has a diameter of 23.38 mm. This is limited by the available space inside the superconducting magnet. The electron gun employed was designed by scaling a Varian MIG by a factor of approximately 0.3. To produce an electron beam of the required radius, it was necessary to have a magnetic compression ratio of about 75. This places the cathode 35 cm from the cavity. As is evident from (3), this creates problems. When the cathode is far away from the cavity, the magnetic field B_c is small. The perpendicular velocity V_{0p} becomes too large even with E_{cp} set at the minimum possible value. This is because the accelerating electric fields which are present outside the cathode region near the mouth of the drift tube also contribute to V_{0p}. The contribution is assumed to be negligible in the adiabatic theory. However, when E_{cp} is small, this contribution becomes significant. The result is reflection of electrons, as they approach the region of high magnetic field near the cavity, similar to that in a plasma mirror machine. The reflected electrons return to the cathode and are reaccelerated by the cathode

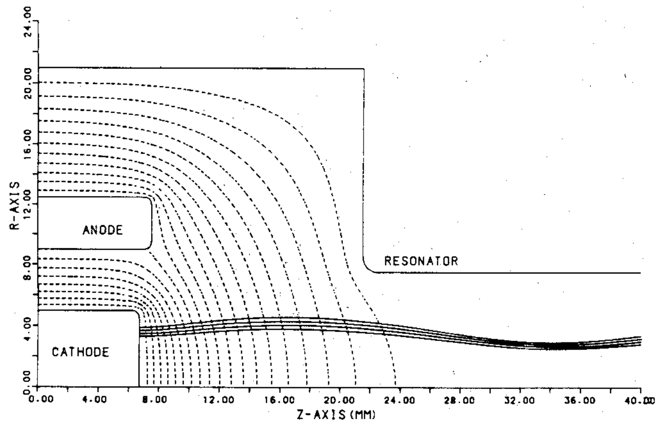

Fig. 2. The cylindrical gun with simulated electron orbits. Conditions are: cathode voltage = −20 kV, anode = −12 kV, cavity magnetic field is 6 T, and the cathode magnetic field 0.08 T. The dotted lines are equipotential surfaces.

potential. Because electron motions at the cathode region are not strictly adiabatic, they have a finite chance of getting through to the cavity.

The normal operating conditions of Gyrotron II as reported in [11] were: electron beam energy 19 kV, anode voltage 16.5 kV, and a magnetic field in the range from 4.5 to 9.5 T. Computation of the electron trajectories under these conditions show that they made multiple reflections between the cavity and the cathode. It is difficult to follow this back and forward motion accurately, but the fact that the gyrotron worked means that eventually enough electrons must have escaped through to the cavity to sustain the gyrotron oscillation. At lower magnetic fields, an auxiliary magnet was required to lower the magnetic compression ratio to make it easier for electrons to get through the magnetic mirror. This is not satisfactory because the transverse velocity of the electron beam cannot be calculated and, hence, the operation of the gyrotron is very unpredictable. There is clearly a need for a new design of the electron gun that can produce the required electron beam without reflections.

III. The New Cylindrical Gun

By increasing the angle of inclination of the cathode emitting surface, the transverse velocity of the electron beam can be decreased. Large inclination guns have been analyzed numerically by Lygin and Tsimring [12]. In our new cylindrical gun, the angle is 90°. A drawing of the electron gun, together with computer simulated electron orbits, is shown in Fig. 2. It is seen that the electric field along the electron trajectories is mainly in the axial direction. The transverse motion of the electrons is caused by the small radial electric field due to the presence of the anode and the mouth of the drift tube. Electron orbits do not cross one another, and the electron beam is laminar. As the electrons move quickly away from the cathode surface, space-charge effects in the cathode region are expected to be small.

In a manner similar to that of the MIG, the cathode–anode voltage difference controls the transverse energy of the electron beam for a fixed beam voltage and magnetic field. However, (3) is not applicable, as E_{cp} is practically zero where the electrons are emitted. The anode controls the transverse energy of the electrons by altering the strength and direction of the electric field. Once the electrons have gained their maximum kinetic energy, they enter the adiabatic compression region, and the transverse velocity increases at the expense of the axial velocity according to (1). The new electron gun is essentially a laminar gun, and (4), which describes the radial position of the electron guiding center, is still applicable.

IV. Computer Simulations of the Broad-Band Behavior of the Cylindrical Gun

As only the transverse energy is useful for interaction, the transverse velocity of the electrons should be as high as possible to ensure high efficiency. A convenient parameter is the velocity ratio

$$W = V_p / V_a \tag{5}$$

where V_a is the axial velocity.

The value of W is limited by the quality of the electron beam, and W achieved by other workers is typically between 1 and 2. It is convenient to characterize the electron beam by the adiabatic invariant $\mu = V_p^2/B$, where V_p is the mean transverse velocity of the electrons. For a fixed-beam energy and cavity magnetic field B_0, there is a maximum value of μ,

$$\mu_{\max} = V_t^2 / B_0 \tag{6}$$

where V_t is the total velocity of the electrons.

If the electron beam produced has a μ larger than $\mu_{\max}$, then reflection will occur. In terms of velocity ratio W, the optimum value of μ is related to $\mu_{\max}$ by

$$\mu = \mu_{\max} W^2 / (W^2 + 1). \tag{7}$$

Thus, for W between 1 and 2, μ is between 50 and 80 percent of $\mu_{\max}$. This is the range of values of μ one usually aims for when designing an electron gun.

Single-electron orbits are calculated by numerically integrating the relativistic Lorentz equation with the electric and magnetic fields closely representing those inside the gyrotron. Space-charge effects are neglected on the grounds that the current density is low. The computer codes which were developed originally to simulate the conventional MIG are easily modified to simulate the cylindrical gun.

A number of representative electrons evenly spaced along the cathode emitting ring are chosen. Electron orbits and velocities are calculated to obtain the mean velocity and velocity spread. The calculation is repeated over the range of magnetic field from 3 T to 12 T. The anode voltage is also varied where appropriate. Fig. 3 shows the parameter μ of the electron beam obtained for different anode voltages as a function of the cavity magnetic field. Throughout the range of magnetic field, it is possible to control the velocity ratio W at the desired value by adjusting the anode voltage alone. The values used in these calculations were chosen to simulate the experimental conditions. With a 9.3-kV electron beam, the maximum transverse velocity spread is predicted to be about 30 percent. However, if the electron-beam energy is increased to 20 kV, the velocity spread can be decreased to no more than 15 percent.

V. Experimental Testing in a Tunable Gyrotron

The cylindrical gun (see Fig. 2) was made to fit inside the Sydney Gyrotron II. The gun consists of a ring of dispenser cathode imbedded in a disc of molybdenum and supported by a heat choke. The anode is in the form of a hollow cylinder. The gun is operated temperature-limited. Control of the cylindrical gun is similar to the old MIG.

Due to the presence of sharp corners in the cathode, which caused electrical breakdown at high voltages, the electron gun was not suitable for operation at voltages higher than ~15 kV. Although computer simulation has shown that the velocity spread

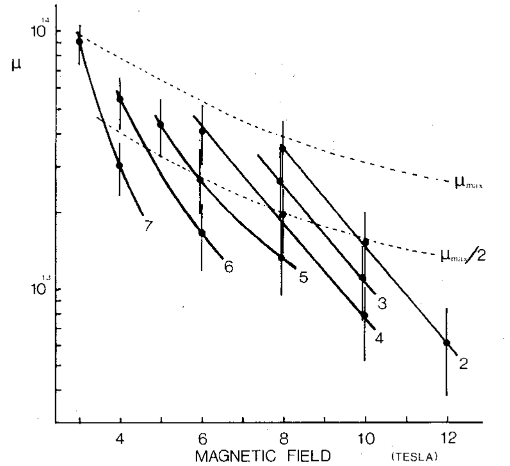

Fig. 3. Computed μ ($= V_{0p}^2/B$) as a function of magnetic field. The cathode voltage is -9.3 kV. The numbers on the curves indicate anode voltages in negative kV. $\mu_{max}/2$ corresponds to a velocity ratio $W = 1$.

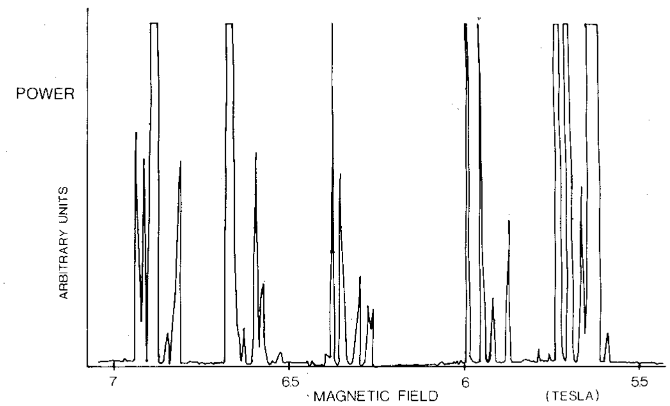

Fig. 4. Gyrotron output power versus magnetic field. Beam voltage is 9.3 kV and current about 80 mA.

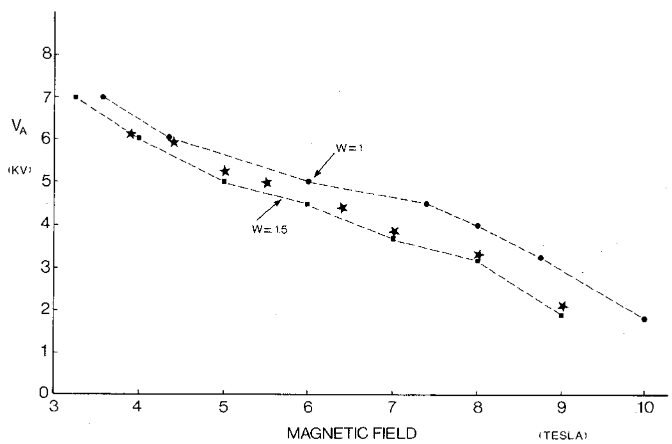

Fig. 5. ★ are the experimental optimum anode voltages versus magnetic field. ● and ■ are the computed data points such that the electron beam has a mean velocity ratio W of 1 and 1.5, respectively.

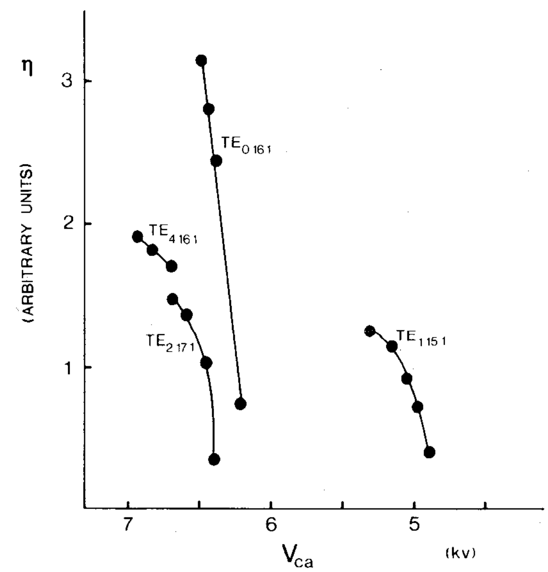

Fig. 6. Relative efficiencies of four gyrotron modes as a function of cathode–anode voltage difference V_{ca}. The value of V_{ca} determined the velocity ratio of the electron beam.

is higher at lower voltages, this did not cause any observable difficulties in the operation of the gyrotron.

A. Wide-Band Operation

The electron-beam voltage was fixed at 9.3 kV and the magnetic field was scanned from 3.5 to 9.0 T. Discrete frequencies corresponding to resonant cavity modes were obtained throughout the whole range. Fig. 4 shows a portion of the output signal as a function of magnetic field. During the scan, as the magnetic field was changed, the anode voltage needed to be adjusted to keep the velocity ratio of the electron beam at the desired level. Fig. 5 shows the anode voltage settings such that the optimum gyrotron signal is generated when the magnetic field is scanned. These voltage settings correspond to a computed velocity ratio W of between 1.0 and 1.5.

The minimum magnetic field used was 3.4 T, and this took the lowest operating frequency of the gyrotron down to 93 GHz. The maximum magnetic field was 9.0 T and the corresponding frequency was 250 GHz.

B. Maximization of Output Efficiency

As only the transverse energy of the electron beam is available for interaction, increasing the proportion of transverse energy can increase the gyrotron efficiency. At a fixed magnetic field, the transverse energy can be increased by an increase in the cathode–anode voltage difference (V_{ca}). Fig. 6 shows the measured relative efficiency of four gyrotron modes as a function of V_{ca}. Gyrotron efficiency was found to increase until a point was reached where electrons were severely reflected and bombarded the electron-gun region, causing the vacuum to degrade and the emission current to be adversely affected.

C. Frequency Measurements and Miscellaneous Observations

Frequencies were measured with a heterodyne receiver which used a stabilized X-band klystron as a local oscillator and with the intermediate frequency displayed on a spectrum analyzer [11]. Simultaneous oscillations of several modes were found to occur much more frequently than when operating with the old electron gun. The beat signals from these modes were observed directly from the spectrum analyzer. Modes with azimuthal numbers 4 and 5 were identified, which were never observed before. The reason was probably due to misalignment of the electron gun. Output power levels were found to be comparable to that obtained with the old electron gun.

VI. Conclusions

A new cylindrical gun has been developed for a low-power tunable gyrotron. In this gun, the electrons are emitted axially rather than radially as in a conventional MIG. Transverse motion of the electrons is caused by the small radial component of the accelerating electric field.

A gun like this would be suitable for any gyrotrons which have very high magnetic compression ratios. Such high-compression ratios may arise in situations like ours where a small electron beam is required. Although the velocity spread in this gun is rather high, for fixed-frequency operations, the electron-beam quality could be improved further by optimization of the anode geometry [12].

The new gun has been tested successfully in a tunable gyrotron and has produced frequencies ranging from 93 to 250 GHz. Controllable and stable operation was possible throughout the whole range of frequencies.

The simple geometry of the cylindrical gun would perhaps allow a grid to be added to make the gun operate in a space-charge limited fashion. A space-charge limited gun would enable the current to be adjusted more readily to control the output power level; this is an advantage to a low-power source for spectroscopic purposes.

Acknowledgment

The author would wish to thank the Beijing Vacuum Electron Devices Research Institute for fabrication of the electron gun. He also acknowledges helpful suggestions from L. C. Robinson, G. F. Brand, and Z. Y. Chen. Special thanks are due to R. G. Hewitt for his advice on the computer simulations. The author would also like to thank colleagues of the gyrotron group for the experimental testing of the electron gun.

References

[1] H R. Jory, "Development of gyrotron power sources in the millimeter wavelength range," in *Proc. Joint Varenna-Grenoble Int. Symp. on Heating in Toroidal Plasmas* (Grenoble, France), July 1978, pp. 351–362
[2] A. V. Gaponov, V. A Flyagin, A. L. Gol'denberg, G. S Nusinovich, Sh. E. Tsimring, V. G. Usov, and S. N. Vlasov, "Powerful millimeter-wave gyrotrons," *Int. J. Electron*, vol. 51, no. 4, pp 277–302, 1981.
[3] Special issue on gyrotrons, *Int. J. Electron*, vol. 53, no. 6, 1982.
[4] M. Caplan and C. Thorington, "Improved computer modelling of magnetron injection gun for gyrotrons," *Int. J. Electron.*, vol. 51, no. 4, pp. 415–426, 1981.
[5] A. W. Fliflet, A. J. Dudas, M. E. Read, and J. M. Baird, "Use of electrode synthesis technique to design MIG-type guns for high power gyrotrons," *Int. J. Electron.*, vol. 53, no. 6, pp. 743–754, 1982.
[6] A. L Gol'denberg and M. I. Petelin, "The formation of helical electron beams in an adiabatic gun," *Radio Phys., Quantum Electron.*, vol. 16, no. 1, pp. 106–111, 1973.
[7] J. D. Jackson, *Classical Electrodynamics* New York: Wiley, 1975, p. 588.
[8] A. L. Gol'denberg and T. B. Pankratova, "Adiabatic theory of electron guns for CRM," (in Russian), *Elektronnaya Tekhnika*, ser. 1, Elektronika SVCh, no. 9, 1971
[9] G. F. Brand, N. G. Douglas, M. Gross, J Y. L. Ma, L. C Robinson, and Chen Zhiyi, "Tunable millimetre-wave gyrotrons," *Int. J. Infrared and Millimeter Waves*, vol. 3, no. 5, pp. 725–734, 1982.
[10] K. E. Kreischer and R. J Temkin, "Linear theory of an electron cyclotron maser operating at the fundamental," *Int. J. Infrared and Millimeter Waves*, vol. 1, no. 2, pp. 195–223, 1980.
[11] G. F. Brand, N. G. Douglas, M. Gross, J. Y. L. Ma, L. C. Robinson, and Chen Zhiyi, "A 125–260-GHz gyrotron," *IEEE Trans. Microwave Theory Tech.*, vol. MTT-32, pp. 58–64, Jan. 1984.
[12] V K. Lygin and Sh. E. Tsimring, "Electron trajectories in helical beams," *Soviet Physics–Technical Physics*, vol 16, no. 11, pp. 1809–1815, Nov 1971.

Probe Mutual Impedance in a Rectangular Waveguide

A. ITTIPIBOON, MEMBER IEEE,
AND L. SHAFAI, SENIOR MEMBER IEEE

Abstract —**The mutual impedance between two probes, arbitrarily located on the broad walls of a rectangular waveguide, is derived by using the reaction concept. This mutual impedance is found to depend on the location and height of the probes and their separation distance. For probes of equal height, it reduces to the probe self impedance, as the probe separation distance approaches zero. The convergence of the solution and the effects of a terminating short circuit on the mutual impedance are also studied and discussed.**

I. Introduction

The problem of post-like structures in a waveguide have been studied by many investigators [1]–[5] who were interested in their equivalent impedance. The equivalent circuits represent a powerful tool for investigation and design of microwave circuits, matching transitions, and various filters. The couplings between waveguide obstacles were studied by Gruenberg [6] for posts of length equal to a waveguide height symmetrically located in the same transverse plane, by Chang and Khan [7] for unsymmetrical cases for posts without gaps, and by El-Sayed [8] for unsymmetrical cases for posts with gaps by using the variational principle. The problem of multipost of the same length equal to a waveguide height and with a gap in each post was studied by Joshi and Cornick [9]–[10]. The structure was considered as a linear N-port network with an impedance matrix obtained by applying the reaction concept. In the present investigation, we are mainly interested in the coupling between two probes arbitrarily located on the broad walls of a waveguide propagating only the dominant mode. The probe impedance as seen by the probe was previously obtained by Lewin [1], [11] and by Collin [12]; however, in this paper, the mutual impedance is obtained by applying the reaction concept [13]. Since the problem in a waveguide is eqivalent to the problem of an antenna radiating in a closed space, the radiation field of the probe can be expanded in terms of the eigenfunctions which form the solution space of the region under consideration. In the present case, the fields will be expanded in terms of the rectangular waveguide modes. The method is general and can be used to solve similar problems in waveguides of different cross sections by selecting their respective eigenfunctions.

Manuscript received August 8, 1984; revised November 13, 1984. This work was supported in part by a grant from the Natural Sciences and Engineering Research Council of Canada.
The authors are with the Department of Electrical Engineering, University of Manitoba, Canada R3T 2N2